Ingenieur-Archiv 53 (1983) 73–83

Ingenieur-Archiv

Creep and Yield in Martensitic Transformations*

M. Achenbach and I. Müller, Berlin

Summary: A model is formulated which simulates the evolution of strain and temperature under dynamic loading in a martensitic transformation. The model describes yielding as a result of a chain reaction between the martensitic transformation and the rise of temperature.

Kriechen und Fließen bei martensitischen Umwandlungen

Übersicht: Es wird ein Modell vorgestellt, welches die Entwicklung der Dehnung und der Temperatur infolge martensitischer Umwandlungen bestimmt. Das Modell beschreibt das Fließen als das Ergebnis einer Kettenreaktion zwischen der martensitischen Umwandlung und der Temperaturzunahme.

1 Introduction

Martensitic transformations, such as they occur in bodies with shape memory, can be effected either by stress or by temperature. Therefore such bodies offer the occasion to study the interaction of mechanical and thermodynamic effects during large deformations.

A model is presented here which simulates the observed stress-strain curves of a body with shape memory as a function of temperature in a quasistatic experiment. In particular the model shows the recovery of a residual deformation at high temperatures.

Simple physical considerations suggest rate laws for the model which predict strain and temperature as functions of time for dynamic loading. With these rate laws the sudden yielding of a body under a critical stress emerges as a consequence of a chain reaction, in which a martensitic transformation creates an increase of temperature and this increase in turn facilitates further transformations. Thus creep and yield occur "automatically", i.e. without the formulation of a specific yield criterion.

The theory presented here is an extension of the calculations in [1], where the same model was treated, but where the implications of the thermomechanical coupling of phenomena not fully recognized.

2 Phenomenology and Model

2.1 Phenomenology of Martensitic Transformation

A body with shape memory at low temperatures has a stress-strain diagram of the form shown in Figure 1a. This is much like the stress-strain diagram of a plastic body except that at large positive and negative values of strain there is an elastic branch along which the body may be loaded far beyond the yield stress σ_y. As the temperature increases the yield stress decreases. At

* This paper was presented at the "Second Symposium on Inelastic Solids and Structures", Bad Honnef, September 1981

high temperatures the body behaves elastically and a typical stress-strain curve is shown in Fig. 1b.

The stress-strain curves of Fig. 1 are valid for static or quasistatic loading at fixed temperatures. They do not reveal how fast the creep proceeds along the yield line or how the strain changes under a prescribed dynamic loading.

The purpose of this paper is the formulation of a model which is capable of simulating the observed behaviour under static loads and in particular the model shall predict a well-defined yield limit. The properties of the model under various dynamic loads will be investigated.

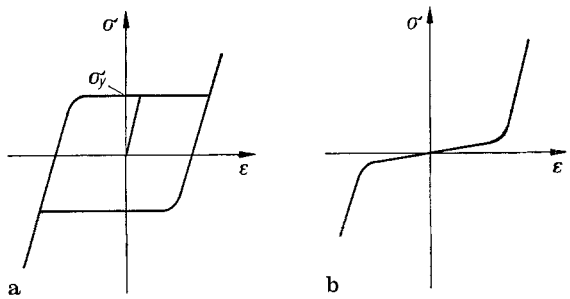

Fig. 1a and **b.** Stress-strain curves at **a** low and **b** high temperatures

2.2 The Model

The basic element of the model is a lattice particle shown in Fig. 2 in its two equilibrium configurations which are denoted by M_+ and M_- thus indicating martensitic twins. The configuration M_+ may be considered as a sheared version of M_- where the shear displacement is J. Values of Δ other than 0 and J are energetically less favourable; indeed we postulate the potential energy $\Phi(\Delta; 0)$ of the lattice particles to have the form shown in Fig. 2. There is an energy barrier between the two potential wells that correspond to M_+ and M_-. For convenience in calculation we simplify this potential and approximate it by two parabolae which meet in a tip at $\Delta = \frac{J}{2}$ as shown by the solid curve in Fig. 3.

Under a prescribed shear force Π the potential energy of the lattice particle is $\Phi(\Delta; \Pi) = \Phi(\Delta; 0) - \Pi\Delta$ since $\Pi\Delta$ is the work done by the force. Thus the curves $\Phi(\Delta; \Pi)$ in Fig. 3 result from adding a straight line $-\Pi\Delta$ to the solid curve $\Phi(\Delta; 0)$. Inspection shows that the load makes the left minimum shallower, while the right minimum becomes deeper. For a critical

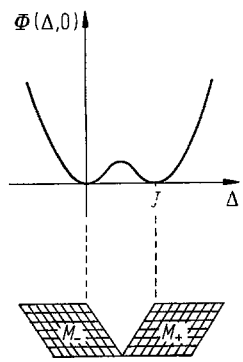

Fig. 2

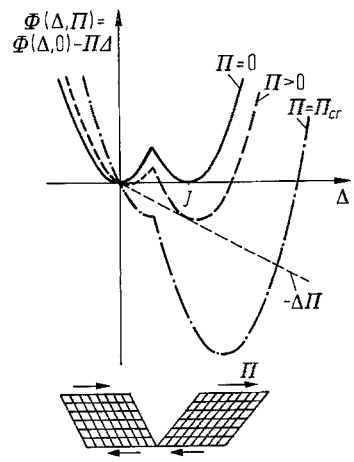

Fig. 3

Fig. 2. Lattice particles and their potential energy
Fig. 3. Lattice particles and their potential under different loads

load Π_{cr} the left minimum vanishes altogether. The formula for the potential reads

$$\Phi(\Delta; \Pi) = \begin{cases} \dfrac{\Pi_{cr}}{J}\Delta^2 - \Pi\Delta & \Delta \leq \dfrac{J}{2}, \\ \text{for} & \\ \dfrac{\Pi_{cr}}{J}(\Delta - J)^2 - \Pi\Delta & \Delta \geq \dfrac{J}{2}. \end{cases} \tag{1}$$

The height of the barrier when approached from the left or right is denoted by B^L and B^R respectively and it is easy to confirm that we have

$$B^L = \frac{\Pi_{cr} J}{4}\left(1 - \frac{\Pi}{\Pi_{cr}}\right)^2 \quad \text{and} \quad B^R = \frac{\Pi_{cr} J}{4}\left(1 + \frac{\Pi}{\Pi_{cr}}\right)^2. \tag{2}$$

The model for the body as a whole is constructed from layers of lattice particles and the layers are stacked as shown in Fig. 4a so that originally M_+ and M_- exist in equal proportions. The construction of this layered model from lattice particles was first proposed in [2]. It is motivate by microscopic observation of the metallic lattice of memory alloys (e.g. see [3]).

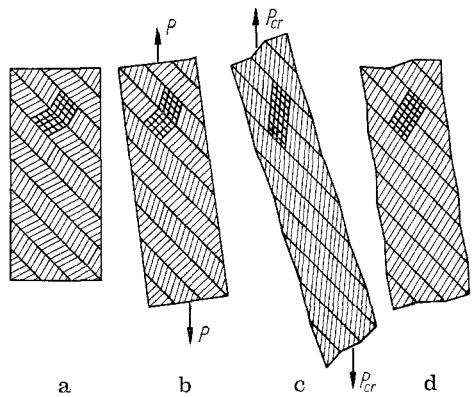

Fig. 4. Model at low temperature under loading

For a simple explanation of how the model simulates yield and residual deformation after unloading we consider first the case of zero temperature. In this case all lattice particles lie in the minima of the potential energy as indicated by the dots in Fig. 5. When a small tensile load P is applied, each lattice particle is sheared by the load

$$\Pi = \frac{1}{\sqrt{2}}\frac{P}{N}, \tag{3}$$

where N is the number of particles in a layer. The potential energy deforms as shown in Fig. 5b; i.e. M_+ particles are made a little flatter and M_- particles become a little steeper as in Fig. 4b. The vertical component of the shear displacement Δ_i of the i^{th} layer ($i = 1, 2, \ldots, n$) contributes to the deformation D so that we have

$$D = \frac{1}{\sqrt{2}}\left(\sum_{i=1}^{n}\Delta_i - \frac{n}{2}J\right).^1 \tag{4}$$

Unloading leads back to the situation of Figs. 4a and 5a which means that small deformations are elastic. When the load P is so big that Π equals Π_{cr}, the M_- particles fall into the M_+ position, because the left minimum is eliminated (see Fig. 5c) and this process is accompanied by a large deformation as shown in Fig. 4c. Unloading now leaves us with a residual deformation, because all layers stay in the M_+ position.

---

1 The constant contribution $-\dfrac{n}{\sqrt{2^3}}J$ in D is chosen so that $D = 0$ holds in the unloaded state when half of the layers are M_+ and the other half M_-

We shall call the fraction of lattice particles in the body the phase factor and denote it by x. Thus $x = 1/2$ in the two configurations of Figs. 4a and 4b, while $x = 1$ in the remaining configurations of Fig. 4. A change of the phase factor x will be called a martensitic transformation.

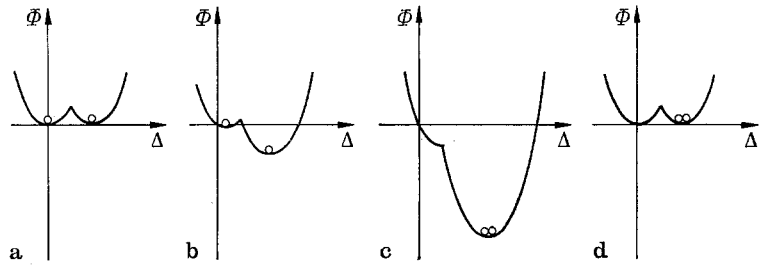

Fig. 5. Potential energy and position of particles at different loads in the case of zero temperature

3 Equations for the Evolution of Deformation, Temperature and Phase Factor for Given Load Functions

3.1 The Effect of Temperature, Transition Probability, and Rate Law for a Transition

At any non-zero temperature the lattice particles do not lie still in their potential wells; rather they fluctuate about the minima and their mean kinetic energy is $1/2\,kT$. The probability $\mathfrak{p}_\Delta^\pm$ for finding a lattice particle $M_\pm$ with the displacement Δ is given by the Eq.

$$\mathfrak{p}_\Delta^\pm = C^\pm \mathrm{e}^{-\frac{\Phi(\Delta;\Pi)}{kT}} \quad \text{for} \quad \begin{matrix} + & \Delta \geq \dfrac{J}{2}, \\ - & \Delta \leq \dfrac{J}{2}. \end{matrix} \tag{5}$$

The constants $C^\pm$ follow from the requirement that

$$\sum_{\Delta=J/2}^{\infty} \mathfrak{p}_\Delta^+ = x \quad \text{and} \quad \sum_{\Delta=-\infty}^{J/2} \mathfrak{p}_\Delta^- = 1 - x.$$

Hence follows

$$\mathfrak{p}_\Delta^+ = x \frac{\mathrm{e}^{-\frac{\Phi(\Delta;\Pi)}{kT}}}{\int\limits_{J/2}^{\infty} \mathrm{e}^{-\frac{\Phi(\Delta;\Pi)}{kT}}\,\mathrm{d}\Delta} \tag{6.1}$$

and

$$\mathfrak{p}_\Delta^- = (1-x) \frac{\mathrm{e}^{-\frac{\Phi(\Delta;\Pi)}{kT}}}{\int\limits_{-\infty}^{J/2} \mathrm{e}^{-\frac{\Phi(\Delta;\Pi)}{kT}}\,\mathrm{d}\Delta}. \tag{6.2}$$

Using these forms for $\mathfrak{p}_\Delta^+$ and $\mathfrak{p}_\Delta^-$ we may rewrite (4) in the form

$$\frac{\sqrt{2}}{nJ} D(\Pi, T, x) = \left\{ x \frac{\int\limits_{J/2}^{\infty} \frac{\Delta}{J} \mathrm{e}^{-\frac{\Phi(\Delta;\Pi)}{kT}}\,\mathrm{d}\Delta}{\int\limits_{J/2}^{\infty} \mathrm{e}^{-\frac{\Phi(\Delta;\Pi)}{kT}}\,\mathrm{d}\Delta} + (1-x) \frac{\int\limits_{-\infty}^{J/2} \frac{\Delta}{J} \mathrm{e}^{-\frac{\Phi(\Delta;\Pi)}{kT}}\,\mathrm{d}\Delta}{\int\limits_{-\infty}^{J/2} \mathrm{e}^{-\frac{\Phi(\Delta;\Pi)}{kT}}\,\mathrm{d}\Delta} - \frac{1}{2} \right\}. \tag{7}$$

Thus the deformation is a function of T, x and of the external load $P = \sqrt{2}\,N\Pi$. Note that for the potential (1) the integrals in the denominator of (7) lead to simple error functions.

As a consequence of the thermal motion the lattice particles may occasionally jump over the barrier between the two potential wells and they will be able to do so more easily the higher the temperature is. Thus a martensitic transformation may occur before the external load has eliminated the barrier.

The rate at which the barrier is overcome is determined by the transition probability of which we have two: one for the jump from left to right and the other one in the opposite direction. We denote these by $\vec{\mathfrak{p}}$ and $\overleftarrow{\mathfrak{p}}$ respectively. We assume that $\vec{\mathfrak{p}}$ is proportional to the probability of lattice particles to lie on the barrier and move to the right. According to (6.2) and since the mean velocity of the lattice particles is given by $\sqrt{\frac{kT}{m}}$, we thus set

$$\vec{\mathfrak{p}} = \sqrt{\frac{kT}{2\pi m}}\,\frac{\mathrm{e}^{-\frac{\Phi(J/2;\Pi)}{kT}}}{\int\limits_{-\infty}^{J/2} \mathrm{e}^{-\frac{\Phi(\Delta;\Pi)}{kT}}\,\mathrm{d}\Delta}. \tag{8}_1$$

By an identical argument we obtain

$$\overleftarrow{\mathfrak{p}} = \sqrt{\frac{kT}{2\pi m}}\,\frac{\mathrm{e}^{-\frac{\Phi(J/2;\Pi)}{kT}}}{\int\limits_{J/2}^{\infty} \mathrm{e}^{-\frac{\Phi(\Delta;\Pi)}{kT}}\,\mathrm{d}\Delta}. \tag{8}_2$$

For the rate law that governs the evolution of the martensitic transformation is assumed to have the simple and self-explanatory form

$$\dot{x} = (1 - x)\,\vec{\mathfrak{p}} - x\overleftarrow{\mathfrak{p}} \tag{9}$$

which implies that the number of particles that leave a potential well is proportional to the number of particles present in that well.

Insertion of the expressions (8) for $\vec{\mathfrak{p}}$ and $\overleftarrow{\mathfrak{p}}$ into the evolution law (9) makes this Eq. specific. We assume that the mean kinetic energy $\frac{1}{2}\,kT$ is much smaller than either B^R or B^L in all cases of interest; therefore we are justified to replace the integrals in (8) by integrals over $-\infty < \Delta < \infty$ provided of course that Φ in $(8)_1$ is taken from $(1)_1$ while Φ in $(8)_2$ is taken from $(1)_2$. The evolution law assumes the form

$$\dot{x} = \frac{1}{\sqrt{2}\pi}\sqrt{\frac{\Pi_{cr}}{mJ}}\left\{(1 - x)\,\mathrm{e}^{-\frac{B^L}{kT}} - x\,\mathrm{e}^{-\frac{B^R}{kT}}\right\}. \tag{10}$$

Note that $\dot{x}$ depends on x, T and Π because B^L and B^R depend on Π as shown in (2).

3.2 Rate Law for Temperature; Chain Reaction

Not only does a high temperature promote martensitic transformations, but in turn a martensitic transformation leads to an increase of temperature, because the lattice particles convert potential energy into kinetic energy when they jump across the barrier into the deep potential well. This is a situation that will lead to a chain reaction unless the kinetic energy thus created is led off by conduction. The reason is simple: The increase of temperature by the martensitic transformation will make further transformations easier which again raise the temperature so that martensitic transformations become still easier, etc., etc.

The formula that governs the growth of temperature reads

$$C\dot{T} = (B^R - B^L)\,v\dot{x} - a(T - T_E), \tag{11}$$

where $\nu = Nn$ is the number of lattice particles in the body, C is the heat capacity, so that $C\dot{T}$ is the rate of change of internal energy. This has two contributions: First there is an increase due to the martensitic transformation, when lattice particles at the rate $\nu\dot{x}$ jump over the barrier and gain the energy $B^R - B^L$. Secondly there is a decrease due to heat-exchange with the environment. This contribution is proportional to the temperature difference between the body and the environment and the factor of proportionality is the heat transfer number a.

3.3 Summary of Equations

The development of the phase factor x and the temperature T for a given external load Π and a given environmental temperature T_E can be calculated from (10) and (11). Once x and T are known as functions of time, the deformation D can be calculated from (7).

For the numerical evaluation of these Eqs. it is useful to introduce dimensionless quantities. We introduce the initial temperature T_I and define:

$$\vartheta \equiv \frac{T}{T_I}, \quad \vartheta_E \equiv \frac{T_E}{T_I}, \quad p \equiv \frac{\Pi}{\Pi_{cr}}, \quad \mathrm{d} \equiv \frac{\sqrt{2}\,D}{n(J/2)}, \quad \varepsilon \equiv \frac{\Pi_{cr} J}{4kT_I}, \quad \gamma \equiv \frac{4k\nu}{C},$$
$$K \equiv \frac{1}{\pi}\sqrt{\frac{\Pi_{cr}}{2mJ}}, \quad \alpha \equiv \frac{a}{C}. \tag{12}$$

With these definitions the differential Eqs. (10) and (11) assume the forms:

$$\dot{x} = K(1-x)\,\mathrm{e}^{-\varepsilon\frac{(1-p)^2}{\vartheta}} - Kx\,\mathrm{e}^{-\varepsilon\frac{(1+p)^2}{\vartheta}}. \tag{13.1}$$

$$\dot{\vartheta} = \gamma\varepsilon p\dot{x} - \alpha(\vartheta - \vartheta_E). \tag{13.2}$$

The Eq. (7) for the deformation reads in dimensionless variables

$$d = p + 2\left(x - \frac{1}{2}\right). \tag{14}$$

We proceed to solve (13) for several choices of parameters and to discuss the resulting qualitative behaviour.

3 4 Discussion of Parameters

While the values of the parameters ε, γ and K reflect properties of the model, like number of layers n, critical load Π_{cr} and jump width J, the parameter α is purely phenomenological. Indeed, α is the ratio of the heat transfer number a and the heat capacity C and from looking at data for metals with a liquid or gaseous environment we may conclude that α is of the order of magnitude of $\frac{1}{\mathrm{sec}}$.

Furthermore K in (13.1) has the dimension of a frequency and it must obviously be interpreted as the frequency with which the lattice particles fluctuate in their potential wells and this will be a big number indeed. We take it to be of the order of magnitude of $10^6\,\frac{1}{\mathrm{sec}}$.

The parameter ε is the ratio of the height of the barrier in the unloaded body and of the mean thermal energy kT_I associated with the initial temperature. This ratio must definitely be greater than 1 and we experiment with values between 20 and 100. Finally, according to the law of Dulong-Petit $C = 3kz$, where z is the number of atoms in the body. Therefore, γ is of the order of magnitude of $\frac{\nu}{z}$, the ratio of the number of lattice particles and of the number of molecules, or, equivalently, γ determines the number of atoms in one lattice particle.

4 Solutions $x(t)$, $\vartheta(t)$ for Given Functions $p(t)$, $\vartheta_E(t)$ for Different Choices of Parameters

4.1 Existence of a Well-Defined Yield Limit

We choose

$$\varepsilon = 100, \qquad \gamma = \frac{4}{3}\frac{1}{10}, \quad \alpha = 0{,}5\,\frac{1}{\text{sec}}, \quad K = 10^6\,\frac{1}{\text{sec}} \tag{15}$$

and prescribe a constant temperature $\vartheta_E = 1$ as well as a load that grows linearly in time to seven different values, namely

$$0.5000,\ 0.5250,\ 0.5500,\ 0.5560,\ 0.5563,\ 0.5570,\ 0.5600$$

and is then held constant. In Fig. 6, top diagram, the resulting deformation is represented as a function of time and we call the attention to the fact, that upon the tiny increase of the load from 0.5560 to 0.5563 the deformation curves change qualitatively from a slow continuous increase to a sudden, "explosive" jump.

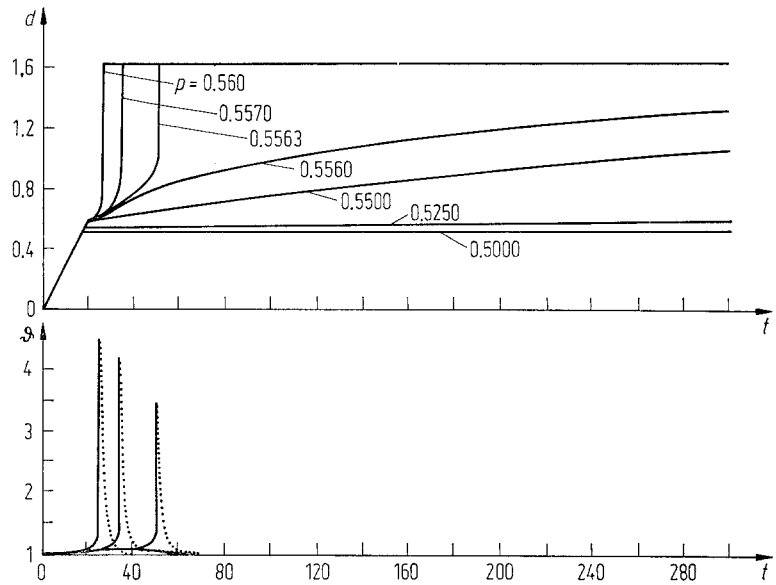

Fig. 6. Deformation d and temperature ϑ as functions of time t; $\varepsilon = 100$; well defined yield limit

We see that at loads below $p = 0.5000$ there is no non-elastic deformation. This range is followed by a narrow range of creep for $0.5000 < p < 0.5560$. Upon a tiny increase of load there follows a range where a sudden yield occurs after an initial creep; the higher the load is the sooner the yield occurs. The yield is the result of the chain reaction whose nature was described in Section 3.2, and it is accompanied, or caused, by a sharp increase of temperature.

The lower diagram of Fig. 6 shows the temperature changes that go along with the evolution of the deformation. There are only small increases of temperature associated with the creep for loads up to $p = 0.55600$, because whatever heat is created by the creep, is led off into the environment. But for larger loads where the sudden yield occurs, we also observe a sharp increase of temperature which is followed by an exponential decay after the maximum deformation is reached, because heat is then led off into the environment.

The remarkable result to be read off from Fig. 6 is that there exists a well-defined yield limit at $p = 0.5560$ without the introduction of a yield criterion.

The parameter $\varepsilon = 100$ has been chosen so big in order to emphasize the possible effects predicted by the Eqs. (13). The effects have thus come out in a rather exaggerated manner. Indeed, the temperature increases more than fourfold when the yield occurs which is certainly quite unrealistic.

The sensitivity of the model to a change of parameter is illustrated by Fig. 7 whose curves refer to $\varepsilon = 25$ with all other parameters as before in (15). Here again we consider a linear increase of the load in time to certain values which are then held constant. Of course, for this smaller value of ε the interesting range of loads lies at smaller values. We observe that the creep region is considerably enlarged, and that the distinction between creep and sudden yield is less clearly identifiable.

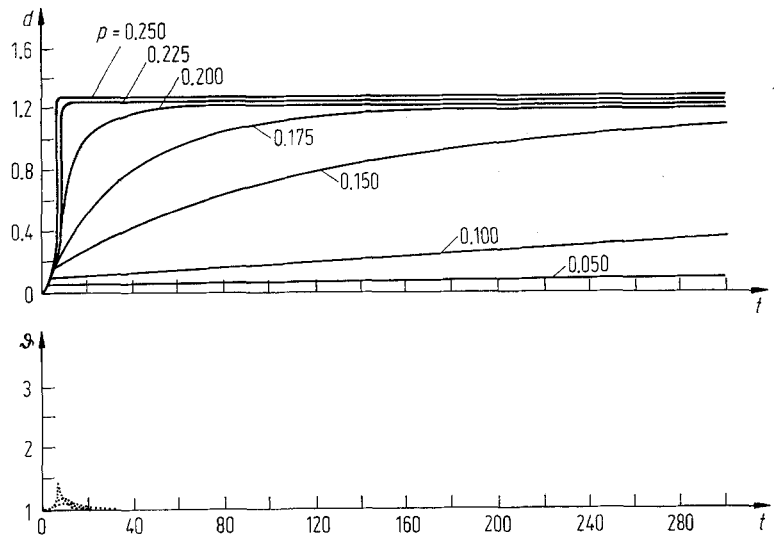

Fig. 7. Deformation d and temperature ϑ as functions of time t; $\varepsilon = 25$; no clear distinction between creep and yield

Indeed there is already creep at $p = 0.050$ and the creep accelerates as p goes up to 0.225. After that, at $p = 0.250$ the yield has occurred, but for the curve deformation vs. time it makes little difference whether there is rapid creep or sudden yield.

The smaller value of ε in Fig. 7 as compared to Fig. 6 entails smaller thermal effects. In the lower part of Fig. 7 the temperatures are drawn as function of t for $p = 0.200$, $p = 0.225$ and $p = 0.250$. We see that, even for $p = 0.250$ the rise of temperature amounts to less than 50% of the initial temperature.

4.2 Sawtooth Load with an Increase of Environmental Temperature

We choose

$$\varepsilon = 25, \quad \gamma = \frac{4}{3}\frac{1}{10}, \quad \alpha = 0.5\,\frac{1}{\text{sec}}, \quad K = 10^6\,\frac{1}{\text{sec}} \tag{16}$$

and prescribe sawtooth loads $p(t)$ with the amplitude 0.3 and the three frequencies

$$f = \frac{1}{80}\frac{1}{\text{sec}}, \quad f = \frac{1}{20}\frac{1}{\text{sec}}, \quad f = \frac{1}{5}\frac{1}{\text{sec}}$$

as shown in Fig. 8a through 8c. In each case the environmental temperature ϑ_E is raised by 50% when the load reaches its maximum the second time.

The Figs. exhibit the calculated behaviour of the phase factor x, the deformation d and the temperature ϑ as functions of time. We observe a sharp increase of x and d as the yield load is surpassed and an accompanying peak in temperature which is more pronounced for higher frequencies than for low ones, because the heat created by the yielding is given less time to flow off.

From the curves $p(t)$ and $d(t)$ we have constructed a load-deformation diagram which is reproduced at the tops of the Figs. 8. We see from this and from the curve $d(t)$ that the model

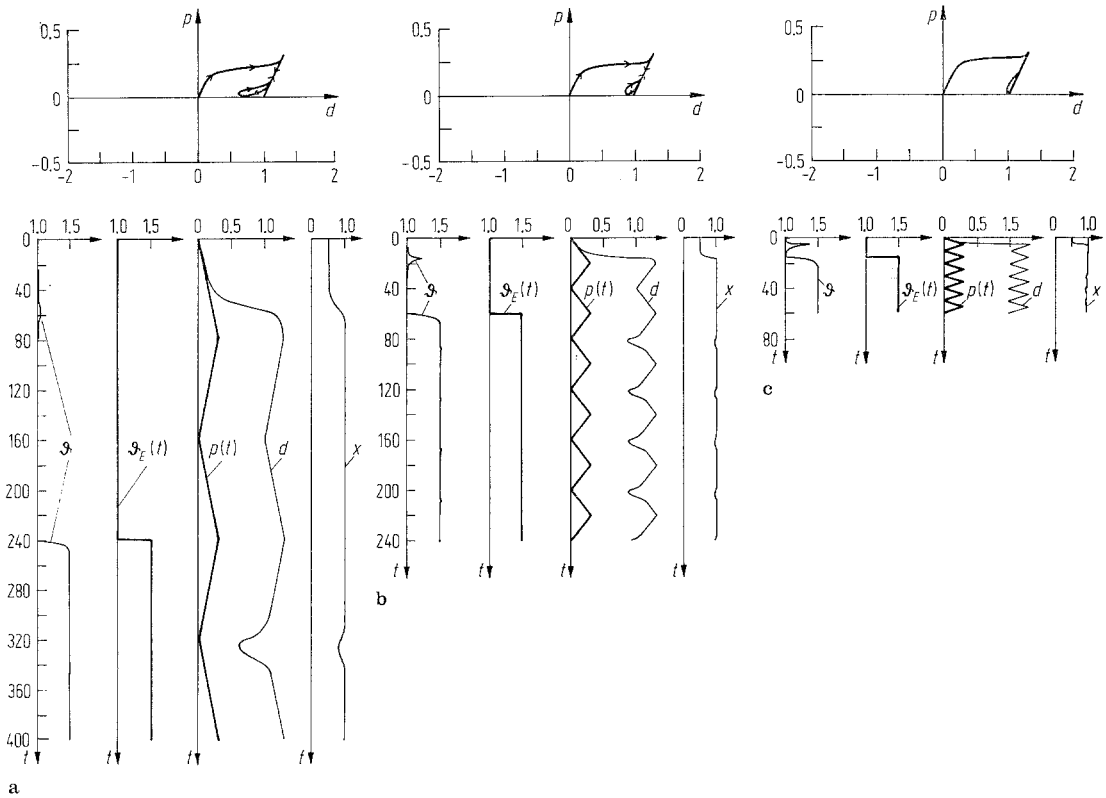

Fig. 8a—c. Sawtooth load with increase of environmental temperature. **a** small frequency of load, **b** intermediate frequency of load, **c** high frequency of load

reaches the right elastic branch corresponding to $x = 1$ on the first loading and remains on that branch during the subsequent process of unloading and reloading. Thus at the low environmental temperature there is a residual deformation, where all lattice particles are of type M_+. After the environmental temperature ϑ_E is increased, the M_+-particles find it possible to jump across the barrier and become M_--particles thus reducing x and d. In this manner the model runs through the loops in the (p,d)-diagrams of the Figs. 8 when the load oscillates. There is partial recovery of the yield at small loads as is appropriate for a model of a memory material. The recovery is more pronounced for small frequencies because it is then given more time.

It must be mentioned that the possibility for the model to recover its yield is strongly dependent on the choice of the parameter ε. Indeed, for the set (15) of parameters including $\varepsilon = 100$ we cannot produce any recovery at all.

4.3 Alternating Load with an Increase of Environmental Temperature

We choose the parameter values (16) and prescribe alternating loads $p(t)$ with the amplitude 0,3 and the two frequencies

$$f = \frac{1}{40}\frac{1}{\text{sec}}, \qquad f = \frac{1}{10}\frac{1}{\text{sec}}.$$

In each case the environmental temperature ϑ_E is again raised by 50% when the load reaches its second maximum.

The Figs. 9 show the (p,d)-diagrams calculated from (13). The initial increase from the origin and the outer hysteresis loop result at the low temperature ϑ_E while the inner hysteresis results at the high environmental temperature. Comparison of the Figs. 9a and 9b shows that both hysteresis loops are narrower for lower frequency. Indeed, we expect that in a quasistatic

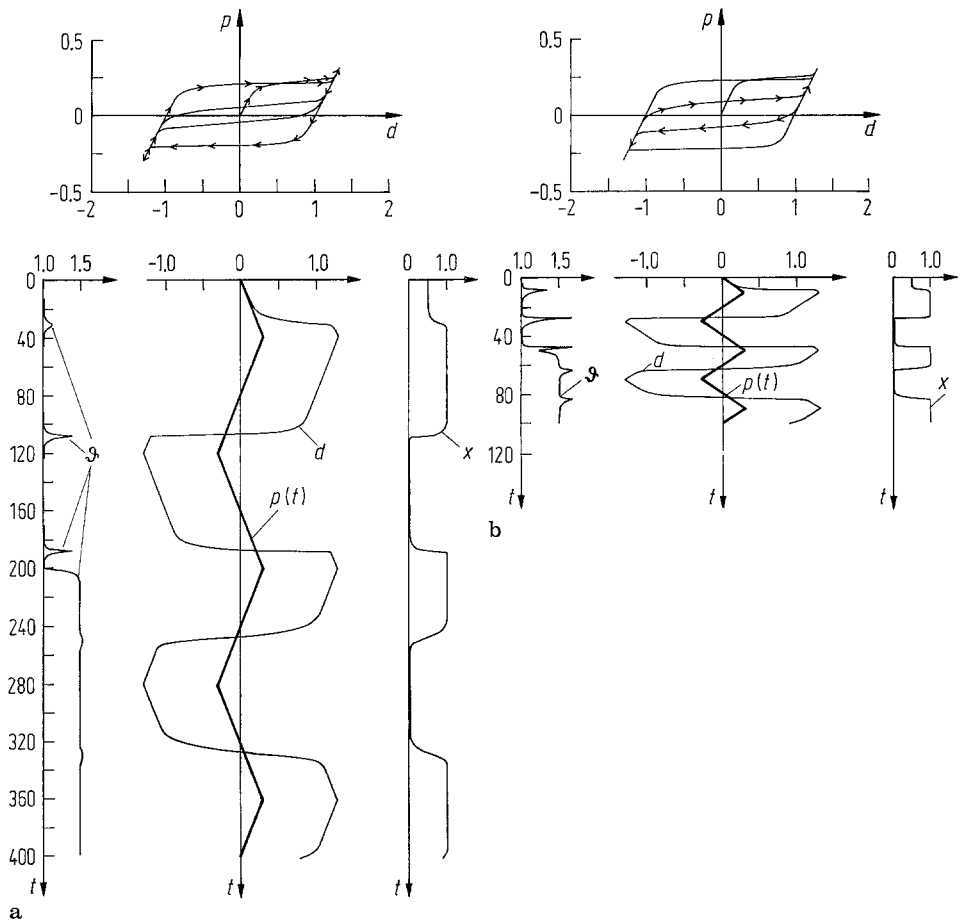

Fig. 9a and **b.** Alternating load with an increase of environmental temperature. **a** small frequency of load, **b** high frequency of load

process at a high temperature the inner hysteresis loop traced out by the model contracts to a single line through the origin as it is observed in materials with shape memory according to Fig. 1b.

4.4 Thermal Effects of Yield and Recovery

When the parameter ε is made smaller, this means that the potential wells of the lattice particles are shallower and therefore yield and recovery are made easier, especially at an elevated environmental temperature. Thus also the thermal effects accompanying yield and recovery are enhanced.

For an illustration of these thermal effects we therefore choose $\varepsilon = 20$ retaining the values (15), or (16) for the other parameters. We apply the sawtooth load of Fig. 8c and increase the temperature ϑ_E by 50% at the time of the second maximum of that load. Figure 10 shows the resulting temperature and we proceed to discuss that curve.

At first, while ϑ_E is still small there is the expected increase of ϑ when the first yield occurs. This is followed by an exponential decay of temperature while the yield-heating flows off. After the increase of ϑ_E the temperature ϑ alternates around this increased value, because the body heats up during the yield and it cools during the recovery of the yield. This cooling is the consequence of a conversion of kinetic energy of the lattice particles into potential energy, because the recovery of yield is effected by the particles' jumping from a deeper potential well to a higher one.

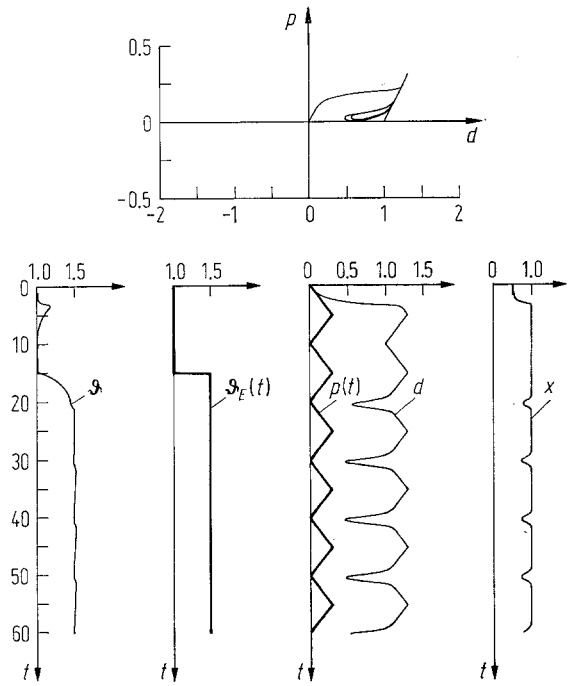

Fig. 10. Thermal effects of yield and recovery

References

1. Achenbach, M.; Müller, I.; Wilmanski, K.: A Model for Creep and Strain Hardening in Martensitic Transformation. J. Therm. Stresses (in press)
2. Müller, I.; Wilmanski, K.: A Model for a Pseudoelastic Body. Nuovo Cimento 57 B (1980) 283–318
3. Cohen, M.; Wayman, C. M.: Fundamentals of Martensitic Reactions. Treatises in Metallurgy (in press)

Received December 1, 1981

M. Achenbach

Prof. Dr. rer. nat. I. Müller
Hermann-Föttinger-Institut für
Thermo- und Fluiddynamik
Technische Universität Berlin
Straße des 17. Juni 135
D-1000 Berlin 12